STIFFNESS-BASED MULTI-REGION 3D BOUNDARY ELEMENT MODELLING OF NON-HOMOGENEOUS SOIL

E. O. A. AZZAM[1], A. F. FARID[2], Y. F. RASHED[3] AND H. A. ELGHAZALY[4]

ABSTRACT

In this paper, a new boundary element technique is presented to predict the settlement and stresses of non-homogeneous soil. Unlike the traditional Boundary Element Method (BEM), the innovative part of the presented formulation is that the soil continuum under arbitrary loadings is divided into boundary element sub-regions, where each sub-region can be regarded as a super finite element. Hence, the stiffness matrix of each sub-region is computed. Such stiffness matrices are computed at interface nodes and are assembled and used to calculate the displacements at interfaces. As a post-processing step, each sub-region is solved separately. Due to the geometrical complexity of the problem, a new preprocessing tool is developed to generate all relevant data. Several numerical examples are solved. The presented technique results are in a good agreement with analytical solution, previously published results and the traditional Finite Element Method (FEM) with less computational effort.

KEYWORDS: Boundary element method, stiffness method, non-homogeneous soil, 3D elasticity

1. INTRODUCTION

Modelling soil as a three-dimensional continuum is essential for complicated and practical problems that appear in reality. Soil problems are huge inherently; therefore, there are several FEM based commercial software packages used to model soil problems such as PLAXIS 3D [1, 2], MIDAS [3, 4], etc. These commercial software packages simulate soil media as finite elements; therefore, it is limited to small or relatively medium problems. As will be demonstrated in section (4), the Finite

---

[1] Assistant Lecturer, Department of Civil Engineering, Fayoum University, Fayoum, Egypt. eoa01@fayoum.edu.eg
[2] Assistant Professor, Department of Structural Engineering, Cairo University, Giza, Egypt.
[3] Professor, Department of Structural Engineering, Cairo University, Giza, Egypt.
[4] Professor, Department of Civil Engineering, Fayoum University, Fayoum, Egypt

Element (FE) discretization is limited to certain level of refinement due to the storage needed. Moreover, its level of accuracy is also limited to a certain level.

Alternative to FEM, simplified models were developed to solve the soil problems. One of these simplified models is Elastic Half Space (EHS) models such as Mindlin [5, 6], Boussinesq [7-9], and Steinbrenner [10, 11]. EHS models consider the soil as infinite elastic and homogeneous continuum. Steinbrenner [10, 11] model can simulate the existence of rigid layer at specific depth. Despite the simplicity of these models, they cannot model the non-homogeneous soil problems.

Other methods are developed to simulate the non-homogeneity of soil in vertical direction such as finite layer method [12-14] and stiffness method [15-17]. The disadvantages of these models are the soil layers must be horizontal layers only and therefore could not simulate general and irregular non-homogeneity of soil.

A new single region BEM has been developed for analyzing the non-horizontally layered half-space where the horizontal boundary surface subjected to tractions [18]. In addition, the soil layers are modeled as parallel layers with a specific inclined angle between the soil surface and the layer's direction. Generalized Kelvin solution was used to eliminate the discretization of internal interface surfaces. In addition, infinite elements were used to take the effect of far fields. It can be seen that this method is limited to problems where all soil layers are parallel.

Mindlin's fundamental solution has been used together with sub-region approach to model two zoned soil only [19]. In addition, infinite elements were used for far field only. The disadvantage of that method is that it fails in case of existence of thin layers as in case of geotextile.

It has to be noted that all these methods have a complicated mathematical model and used to solve a special cases of non-homogeneity in addition; the need of infinite element within the context of BEM gains too little improvements. Therefore, it is not applicable for practical problems where irregular non-homogeneity appears. Therefore, there is a need to develop a methodology to simulate soil problems with arbitrary non-homogeneity as the case of FEM together with less storage and high accuracy of the BEM.

Therefore, in this paper, a 3D multi-region analysis using stiffness based boundary element method is developed. The soil media is divided into boundary element sub-regions with zero Dirichlet boundary condition in the far fields. Each sub-region can be regarded as super finite element and stiffness analysis is used to solve the overall problem.

Most of the open source preprocessing programs are FE oriented programs, therefore a new boundary element preprocessing program is developed to generate all relevant problem information in the desired format. Numerical examples are presented and results are compared to previously published results. The results demonstrate the validity of the proposed technique.

2. THE PROPOSED FORMULATION

In this section, analysis of general non-homogeneous soil media using the proposed three-dimensional boundary element formulation is presented. Generally, soil continuum is discretized into 3D sub-regions (N_n) as shown in Fig. 1 and is modeled as 3D boundary element method. Load vector and stiffness matrix of each sub-region is extracted as presented in the next sub-sections. Hence, assembly procedure is proposed to solve the overall system. It has to be noted that each sub-region could be regarded as super finite element and this is the main idea of the proposed formulation.
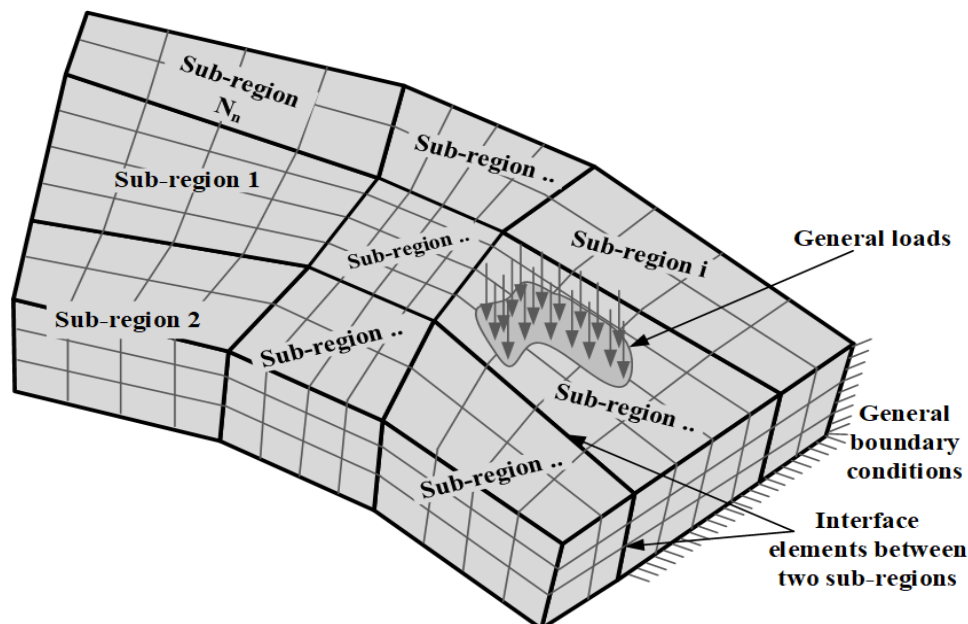

Fig. 1. The considered soil continuum discretized into N_n sub-regions.

2.1 Sub-region Boundary Element Formulation

Consider a general 3D sub-region boundary Γ as shown in Fig. 2. The indicial notation is used, where the Roman indices vary from 1 to 3. The relevant integral equation could be written as follows:

$$C_{ij}(\xi)u_j(\xi) + \int_{\Gamma(x)} T_{ij}(\xi,x)u_j(x)d\Gamma(x) = \int_{\Gamma(x)} U_{ij}(\xi,x)t_j(x)d\Gamma(x) \qquad (1)$$

Where $T_{ij}(\xi, x)$, $U_{ij}(\xi, x)$ are the two-point fundamental solution kernels for tractions and displacements respectively [20]. The two points ξ and x are the source and the field points respectively. $u_j(x)$ and $t_j(x)$ denote the boundary generalized displacements and tractions. $C_{ij}(\xi)$ is the free term. After discretizing the boundary of the region into N_e linear surface boundary elements, Eq. (1) could be re-written in a matrix form as follows:

$$\begin{matrix} & 3N_I & 3N_g \\ \begin{matrix} 3N_I \\ 3N_g \end{matrix} & \begin{bmatrix} H_1 & H_2 \\ \hdashline H_3 & H_4 \end{bmatrix} \end{matrix} \times \begin{matrix} 3N_I \\ 3N_g \end{matrix} \begin{Bmatrix} u_I \\ \hdashline u_g \end{Bmatrix} = \begin{matrix} 3N_I \\ 3N_g \end{matrix} \begin{matrix} & 3N_I & 3N_g \\ & \begin{bmatrix} G_1 & G_2 \\ \hdashline G_3 & G_4 \end{bmatrix} \end{matrix} \times \begin{matrix} 3N_I \\ 3N_g \end{matrix} \begin{Bmatrix} t_I \\ \hdashline t_g \end{Bmatrix} \qquad (2)$$

Where, N_I and N_g are the numbers of interface and general nodes respectively. $[H]$ and $[G]$ are the well-known influence matrices. The vectors $\{u_I\}$, $\{u_g\}$, $\{t_I\}$ and $\{t_g\}$ are the interface nodal displacements, general nodal displacements, interface nodal tractions, and general nodal tractions respectively.
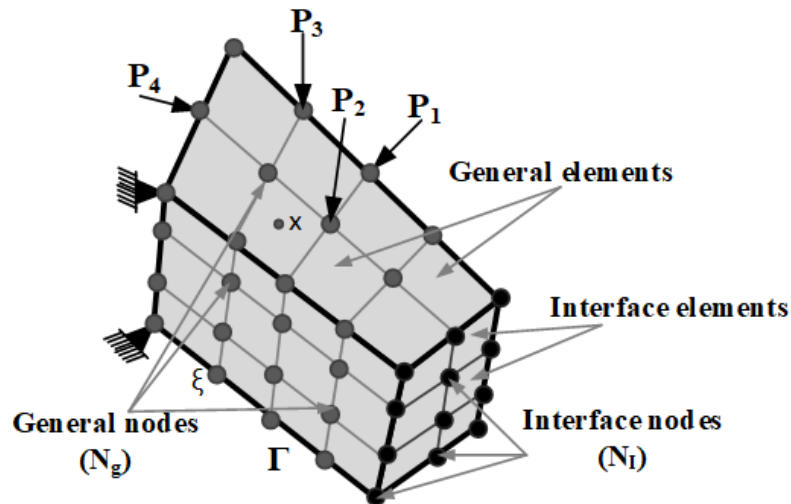

Fig. 2. Surface discretization of an arbitrary 3D boundary element sub-region.

2.2   Computation of Sub-region Stiffness Matrix

In this section, Eq. (2) is re-used to extract the stiffness matrix of each sub-region. Stiffness matrix of the sub-region is extracted at the degrees of freedom of interface nodes ($3N_I$). In order to force $\{t_I\}$ to represent the stiffness matrix, $3N_I$ cases of loading are considered. Each considered load case is set to have a unit generalized displacement in a single degree of freedom and zeros at the other degrees of freedom. That means, the vector $\{u_I\}$ is replaced by a matrix $[u_I]$ with size $3N_I$ x $3N_I$ and is forced to be the unity matrix $[I]$, as follows:

$$
\begin{array}{cc} & \begin{array}{cc} 3N_I & 3N_g \end{array} \end{array}
\begin{array}{c} 3N_I \\ 3N_g \end{array}
\begin{bmatrix} H_1 & H^*_2 \\ H^*_3 & H^*_4 \end{bmatrix}
\times
\begin{array}{c} 3N_I \\ 3N_g \end{array}
\begin{array}{c} 3N_I \\ \end{array}
\begin{bmatrix} I \\ B \end{bmatrix}
=
\begin{array}{c} 3N_I \\ 3N_g \end{array}
\begin{array}{cc} 3N_I & 3N_g \end{array}
\begin{bmatrix} G_1 & G^*_2 \\ G^*_3 & G^*_4 \end{bmatrix}
\times
\begin{array}{c} 3N_I \\ 3N_g \end{array}
\begin{array}{c} 3N_I \\ \end{array}
\begin{bmatrix} K \\ C \end{bmatrix}
\tag{3}
$$

Where $[K]$ is the required sub-region stiffness matrix. It has to be noted that, general nodes could have prescribed displacements or tractions. Therefore, the influence matrices $[H]$ and $[G]$ are reordered to force the matrices $[B]$ and $[C]$ to be the known and unknowns values respectively. H^*_2, H^*_3, H^*_4, G^*_2, G^*_3, and G^*_4 are the new influence matrices after re-ordering the general degrees of freedom. It can be seen from Eq. (3) that each column of the matrix $[C]$ represents the unknown displacements $\{u_g\}$ and tractions $\{t_g\}$ of general nodes corresponding to the associated stiffness cases. This matrix will be re-used in the post-processing stage. Stiffness matrix of the sub-region interface nodes degrees of freedom $[K]$ and the corresponding general nodes displacements and tractions values corresponding to the associated stiffness cases $[C]$ can be computed by solving Eq. (3).

2.3   Computation of Sub-region Load Vector

In order to obtain the sub-region load vector at interface nodes degrees of freedom, all interface displacements are set to be zeros, therefore Eq. (2) is re-written as follows:

$$
{}^{3N_I}\begin{bmatrix} \overset{3N_I}{H_1} & \overset{3N_g}{H_2} \\ \hline H_3 & H_4 \end{bmatrix}^{3N_g} \times {}^{3N_I}_{3N_g}\begin{Bmatrix} 0 \\ \hline u_g \end{Bmatrix} = {}^{3N_I}_{3N_g}\begin{bmatrix} \overset{3N_I}{G_1} & \overset{3N_g}{G_2} \\ \hline G_3 & G_4 \end{bmatrix} \times {}^{3N_I}_{3N_g}\begin{Bmatrix} t_I \\ \hline t_g \end{Bmatrix} \tag{4}
$$

Recalling that the general nodes could have prescribed displacement or traction values, Eq. (4) is re-ordered and re-written as follows:

$$
{}^{3N_I}_{3N_g}\begin{bmatrix} \overset{3N_I}{H_1} & \overset{3N_g}{H^*_2} \\ \hline H^*_3 & H^*_4 \end{bmatrix} \times {}^{3N_I}_{3N_g}\begin{Bmatrix} 0 \\ \hline b_g \end{Bmatrix} = {}^{3N_I}_{3N_g}\begin{bmatrix} \overset{3N_I}{G_1} & \overset{3N_g}{G^*_2} \\ \hline G^*_3 & G^*_4 \end{bmatrix} \times {}^{3N_I}_{3N_g}\begin{Bmatrix} t_{I0} \\ \hline x_{g0} \end{Bmatrix} \tag{5}
$$

Where, $\{b_g\}$ is a known vector of the prescribed tractions or displacements. $\{t_{I0}\}$ and $\{x_{g0}\}$ are the tractions at the fixed interface nodes due to region loads (which is the required load vector) and the unknown vector at general region nodes respectively.

2.4   Analysis of Overall Soil Continuum

Once the stiffness matrix $[K]$ and the load vector $\{t_{I0}\}$ of each sub-region are computed (recall Eqs. (3, 5)), assembly procedure is performed to form the global stiffness matrix and load vector of the non-homogeneous soil continuum at the interface degrees of freedom. Overall system equilibrium equation could be written as follows:

$$
{}^{3N_{It}}\!\begin{bmatrix} \overset{3N_{It}}{K_{all}} \end{bmatrix} \times {}^{3N_{It}}\{u_{all}\} = {}^{3N_{It}}\{P_{all}\} \tag{6}
$$

Where, $[K_{all}]$, $\{u_{all}\}$, and $\{P_{all}\}$ are the overall stiffness matrix, unknown displacements, and load vector of all interface degrees of freedom of the overall media respectively. It can be seen that such assembly procedure is similar to the well-known finite element procedures which makes the presented formulation is very versatile to be linked with FEM. It has to be noted that N_{It} is the total number of interface nodes

between all sub-regions of the soil continuum. By solving Eq. (6), the displacements at interface nodes are computed.

2.5 Sub-region Post-processing Stage

In the post-processing, tractions and displacements at any sub-region node on the boundary (general or interface node) could be computed as follows:

$$
\begin{array}{c} 3N_I \\ 3N_g \end{array} \left\{ \begin{array}{c} t_I(j) \\ x_g(j) \end{array} \right\} = \begin{array}{c} 3N_I \\ 3N_g \end{array} \left\{ \begin{array}{c} t_{I0}(j) \\ x_{g0}(j) \end{array} \right\} + \begin{array}{c} 3N_I \\ 3N_g \end{array} \left[\begin{array}{c} K(j) \\ \hline C(j) \end{array} \right]^{3N_I} \times \begin{array}{c} 3N_I \end{array} \left\{ u_I(j) \right\} \tag{7}
$$

Where, the index j denotes the sub-region number and vary from 1 to N_n. In addition, post-processing can be performed to evaluate any internal point at any sub-region using the integral Eq. (1), in which the matrix form in this case could be written as follows:

$$
3N_{int} \left\{ u_{int} \right\} + 3N_{int} \begin{array}{cc} 3N_I & 3N_g \\ \left[H_5 \, H_6 \right] \end{array} \times \begin{array}{c} 3N_I \\ 3N_g \end{array} \left\{ \begin{array}{c} u_I \\ \hline u_g \end{array} \right\} = 3N_{int} \begin{array}{cc} 3N_I & 3N_g \\ \left[G_5 \, G_6 \right] \end{array} \times \begin{array}{c} 3N_I \\ 3N_g \end{array} \left\{ \begin{array}{c} t_I \\ \hline t_g \end{array} \right\} \tag{8}
$$

Where, H_5, H_6, G_5, G_6 are new influence matrices between the internal points (N_{int}) and the other nodes. $\{u_{int}\}$ is displacement vector of internal points.

3. THE DEVELOPED PREPROCESSING TOOL

Although there are a number of open source FE oriented programs that perform the meshing process for a three-dimensional problems such as the Gmsh [21], there is a need to perform the meshing with a different orientation to be compatible with the requirements of solving a 3D Boundary Element (BE) problem (as the problems considered herein). In multi-region 3D BE problems, the contact surfaces must be discretized with a specific way as shown in Fig. 3, where the matching nodes must have the same number and the element nodes incidence depends on the type of relevant region. In this section, a new 3D Boundary Element Preprocessing Program (BEPP) has been developed to configure all relevant data to the developed program with the desired way.
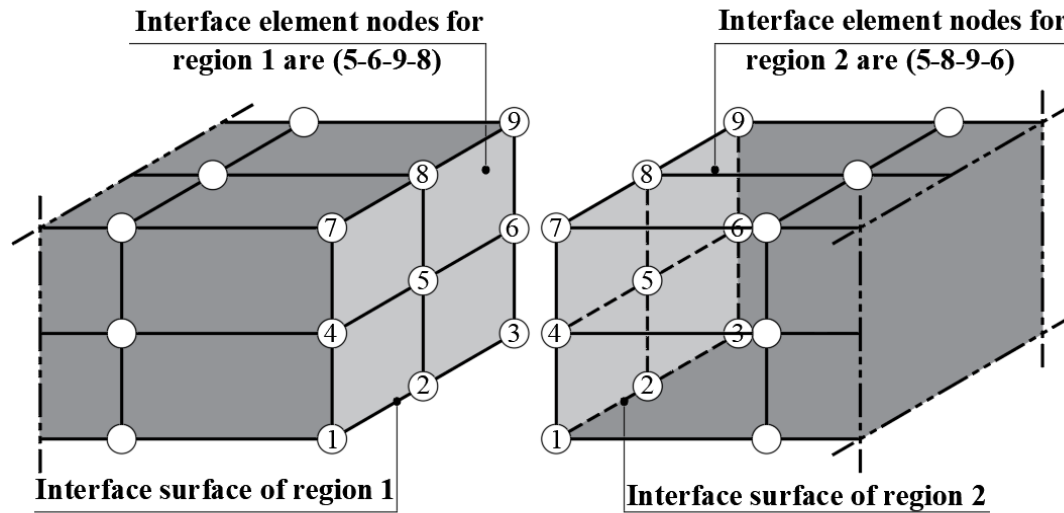
Fig. 3. Soil continuum discretized using transition elements.

The BEPP generates all the needed element information such as, element's nodes incidence, element's node coordinates, and region's elements number. In addition, transition elements could be used to change the number of division in the loaded sub-region surfaces from other sub-region surfaces. This change is applicable in both horizontal and vertical directions as shown in Fig. 4.

It has to be noted that, using BEPP, the prescribed values of Dirichlet and Neuman BC can be assigned to sub-region surfaces. Hence, the prescribed values of elements BC could be extracted automatically.

4.   NUMERICAL EXAMPLES

In order to verify the proposed BE formulation, a computer program has been written using FORTRAN code. Three numerical examples are solved. Results of the first two examples are compared to the previously published results and the results of the third example are compared to analytical solution.
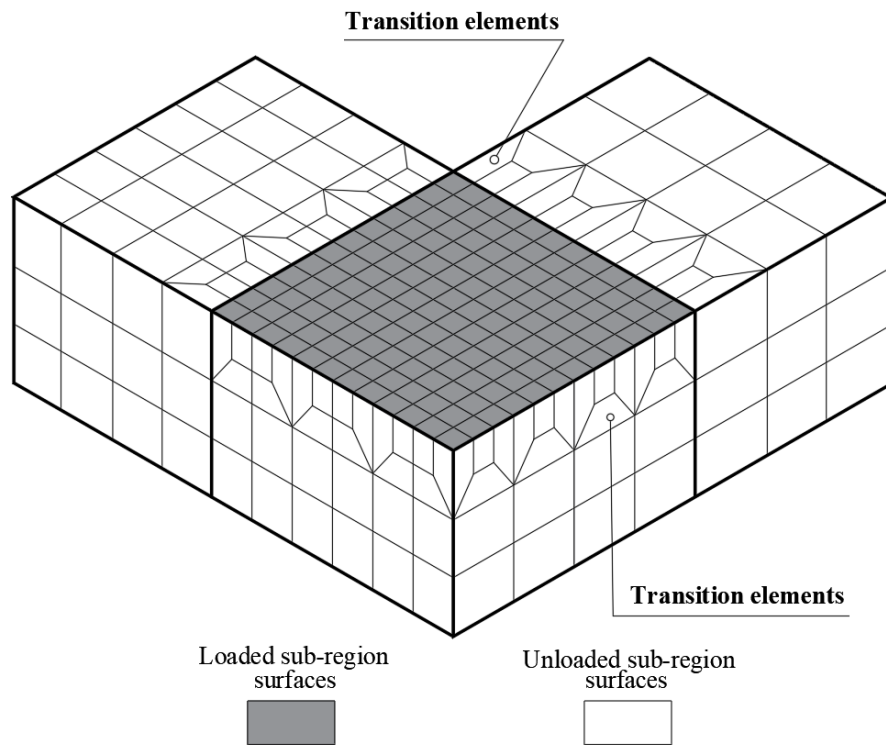
Fig. 4. Two interface surfaces discretized with the desired way using the developed BEPP.

4.1 Square Loaded Area on Half Space with Two Different Soil Types

In this example, a square area of dimensions (2m × 2m) over elastic half space with two different soil types is solved. The modulus of elasticity is 10,000 kN/m^2 and 2,000 kN/m^2, respectively, and the Poisson's ratios are equal to zero for the two soils as shown in Fig. 5. The interface plane is inclined by 45° with the horizontal surface. The loaded area is subjected to pressure equals to 100 kN/m^2.

This example is solved using the proposed BE technique and using the traditional 3D Finite Element Method (FEM). In the BE model, the size of element under the loaded area is 1m × 1m and the surrounding edge distance is 20m away from the end of loaded area with zero Dirichlet BC . Rigid layer is located at depth of 16m as shown in Fig. 6.

In the FEM, three-different models are considered. Each model has different element size under the loaded area, that is: 1m × 1m, 0.5m × 0.5m, and 0.25m × 0.25m, respectively. All FE models have the same boundary conditions as those in BE model. In addition, the FE model 1m × 1m, discretization has the same boundary discretization

that in the BE model as illustrated in Fig. 6. The discretization has been doubled for the other FE models. The 3D FE used in these models is, eight-noded solid quadrilateral element. The results of the presented BE technique and the results of the FEM are compared to previous results [18, 19] as shown in Table1 and the errors have been computed relative to the results of these two references.

It can be seen that, the present BE results are in very good agreement with previously published results and more accurate than those of the FEM results. In addition, it was difficult to use smaller element to (0.25m × 0.25m) in the used FEM because of the storage requirements.
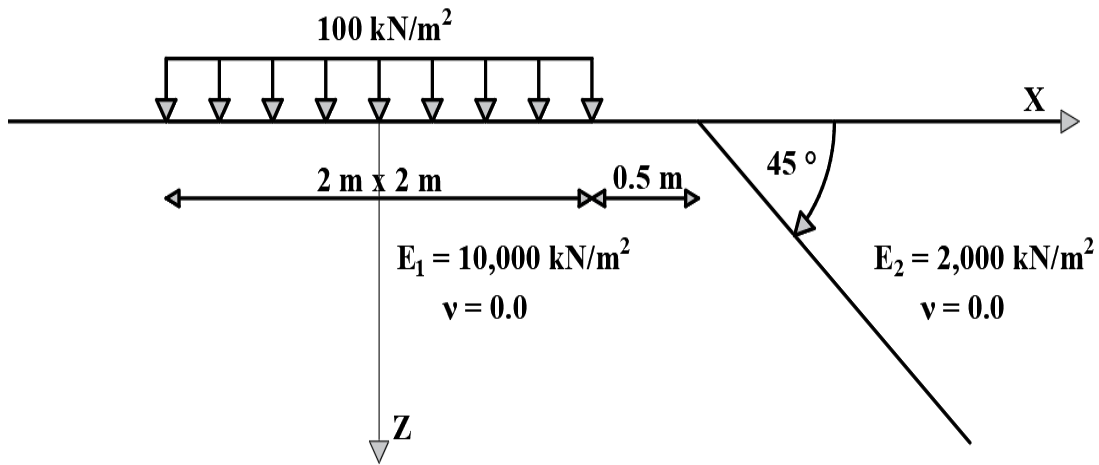
Fig. 5. Square loaded area on two different soils in example 4.1.
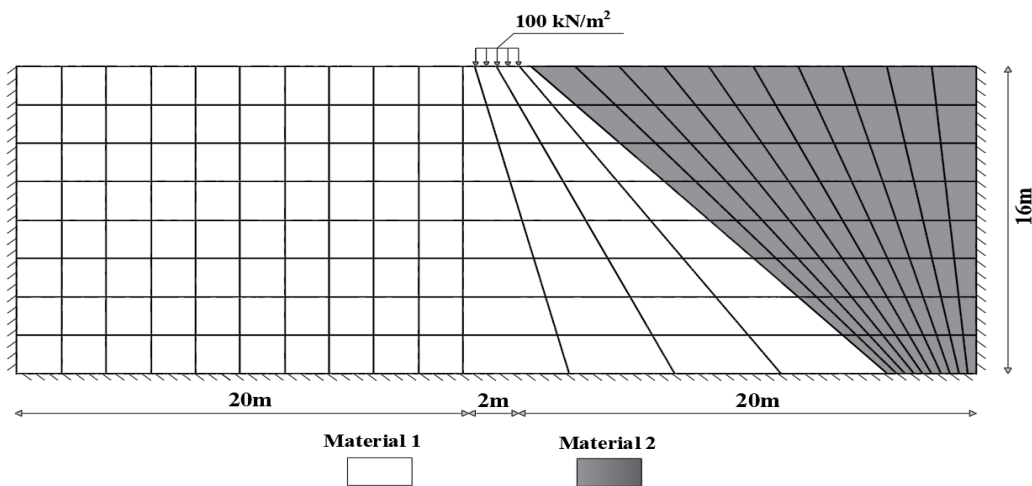
Fig. 6. Boundary element model for square loaded area on two different soils.

Table 1. Displacements (m) at the center and corners of square loaded area on elastic half space two different soils in example 4.1.

	[18]	[19]	Present BEM Mesh 1m×1m	3D FEM Mesh 1m×1m	3D FEM Mesh 0.5m×0.5m	3D FEM Mesh 0.25m×0.25m
Center (m)	0.0229	0.022428	0.02267	0.02097	0.021	0.0214
Error, % [18]			1 %	8.5 %	8.3 %	6.55 %
Error, % [19]			1.1 %	6.5 %	6.37 %	4.58 %
Corners near interface, m	0.011405	0.011216	0.01187	0.01086	0.01091	0.0105
Error, % [18]			4.08 %	4.8 %	4.34 %	7.94 %
Error, % [19]			5.8 %	3 %	2.55 %	6.38 %
Other corners, m	0.011233	0.011195	0.01142	0.01086	0.01088	0.0103
Error, % [18]			1.7 %	4.8 %	3.14 %	8.3 %
Error, % [19]			2 %	3 %	2.81 %	7.99

4.2 Square Loaded Area on a Half Space with Three Different materials (Rock)

In this example a square area of dimensions (2m×2m) is loaded over elastic half space with three different materials (Rock) as shown in Fig. 7. The modulus of elasticity is 20,000 MPa, 40,000 MPa, and 20,000 MPa, respectively. The Poisson's ratios are equal to 0.3, 0.25, and 0.3, respectively. The two interface planes are 90° with the horizontal surface. The loaded area is subjected to pressure equals to 100 MPa.
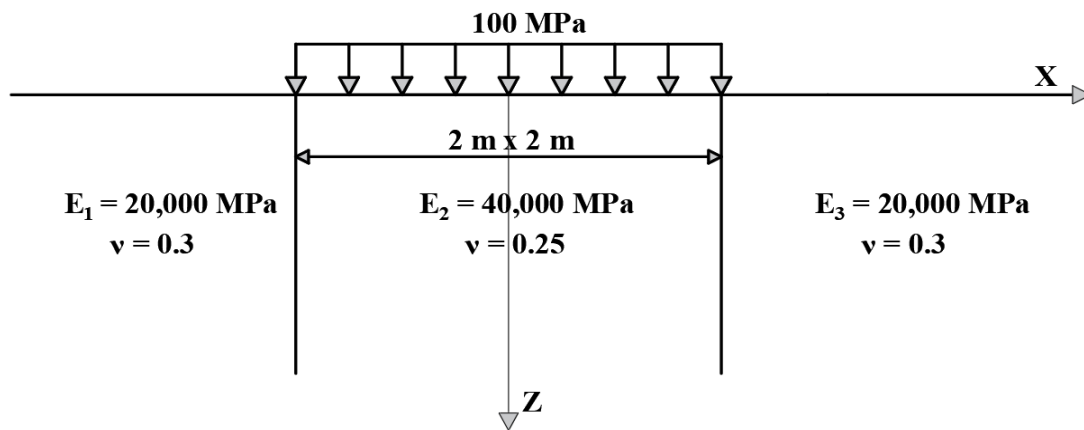

Fig. 7. Square loaded area on three different materials (Rock) in example 4.2.

The BE model is generated by BEPP as shown in Fig. 8. The number of divisions under the loaded area is 16×16 and have been reduced in the far zones as shown in Fig.

8. The surrounding edge distance is 16m away from the end of loaded area with zero Dirichlet BC. Rigid layer is located at depth of 16m.
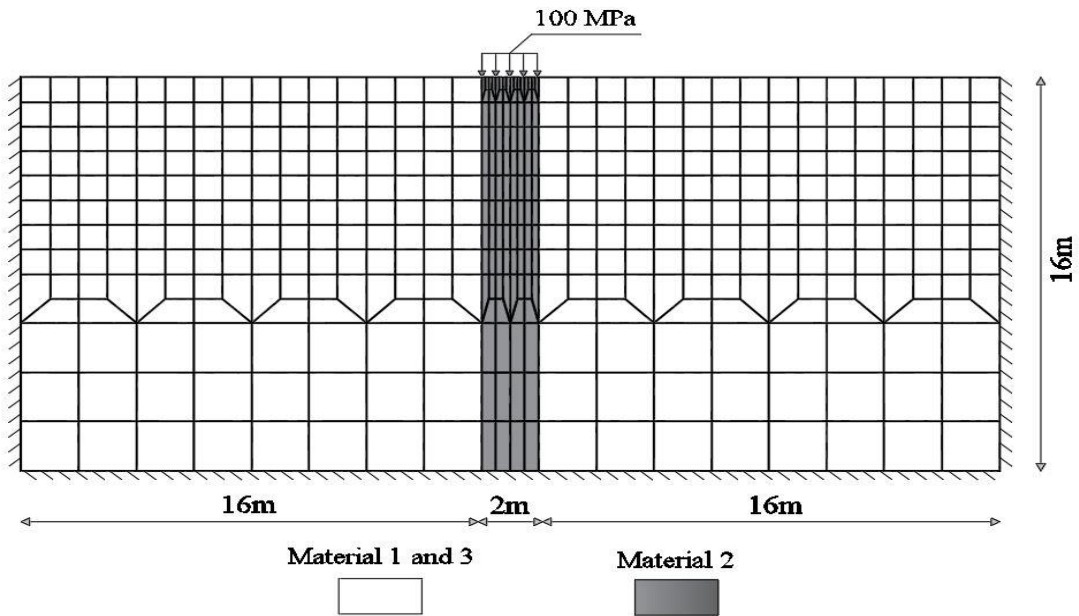

Fig. 8. Boundary element model for the square loaded area in example 4.2.

Figures 9 and 10 demonstrate displacements and stresses along horizontal strip under the loaded area respectively. It can been seen that, results are in a very good agreement with previously published results [18].
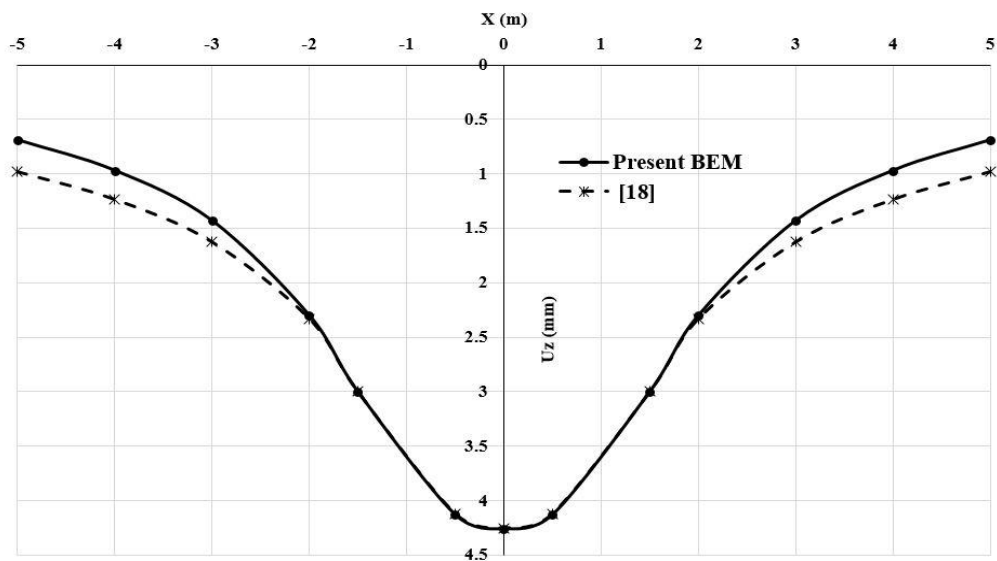

Fig. 9. Displacements (U_z) along strip under the loaded area
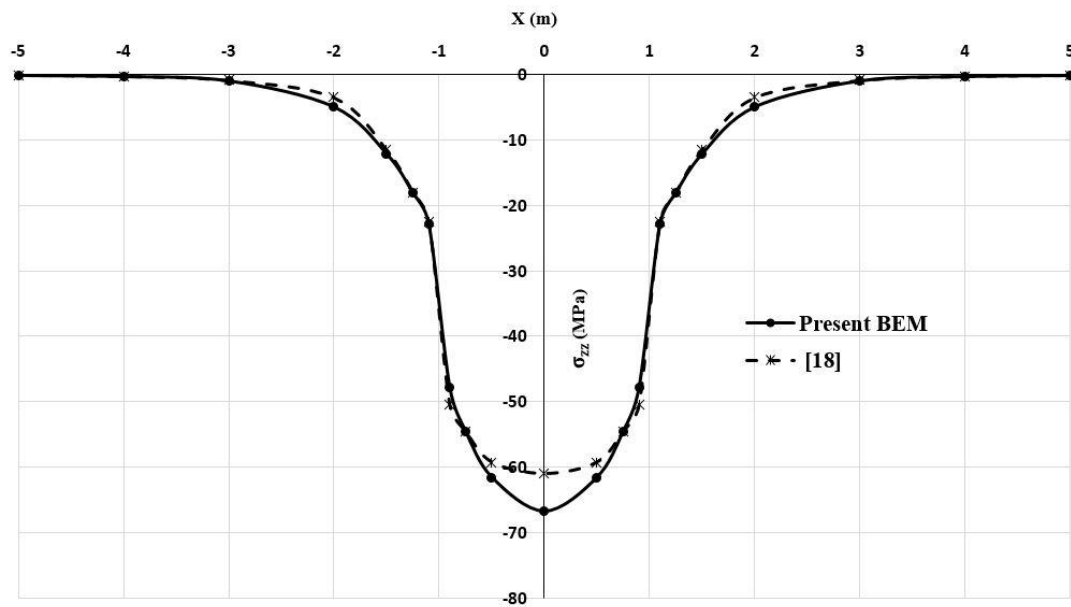at y=0.5m and z=1m in example 4.2.

Fig. 10. Stresses (σ_{zz}) along strip under the loaded area at y=0.5m and z=1m in example 4.2.

4.3 Square Loaded Area on a Homogenous Elastic Half Space

In this example, a square loaded area of dimensions (2m×2m) over a homogenous elastic half space shown in Fig. 11 is solved. The modulus of elasticity and the Poisson's ratio of the EHS are 10,000 kN/m² and zero respectively. The loaded area is subjected to a uniform pressure equals to 100 kN/m².
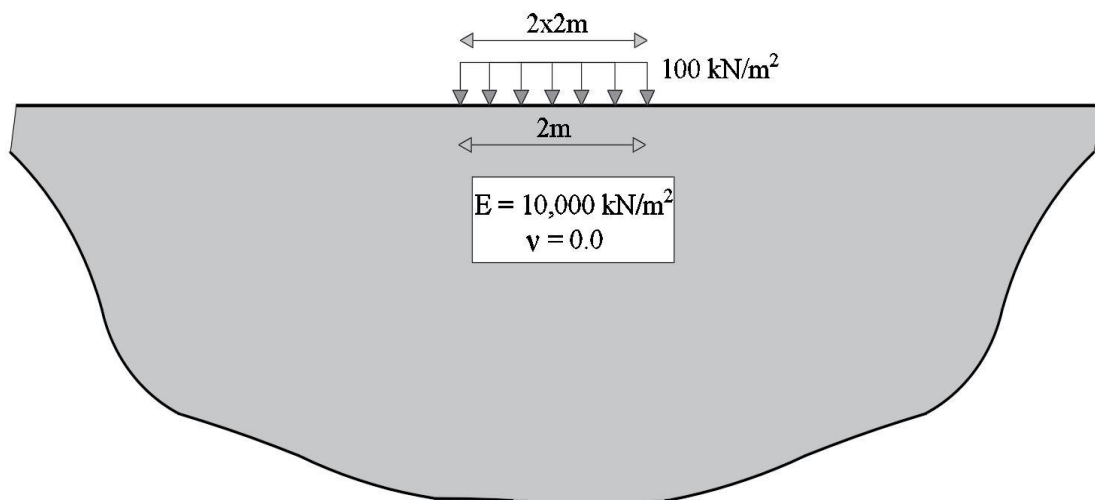

Fig. 11. Square loaded area on a homogeneous elastic half space in example 4.2.

This example is solved using the proposed technique and using the traditional 3D FEM. The BE model, is the same as in example 4.1 with the same discretization and BCs as shown in Fig. 6.

In the FEM, three-different models are considered. Each model has a different mesh size, that is: medium, fine, and very fine. All FE models have the same boundary conditions as those in BE model. The FE model of very fine mesh size is illustrated in Fig. 12 where, ten nodes quadratic tetrahedral element is used. The results of the presented technique and the results of the FEM are compared to analytical solution [22] as shown in Table 2.
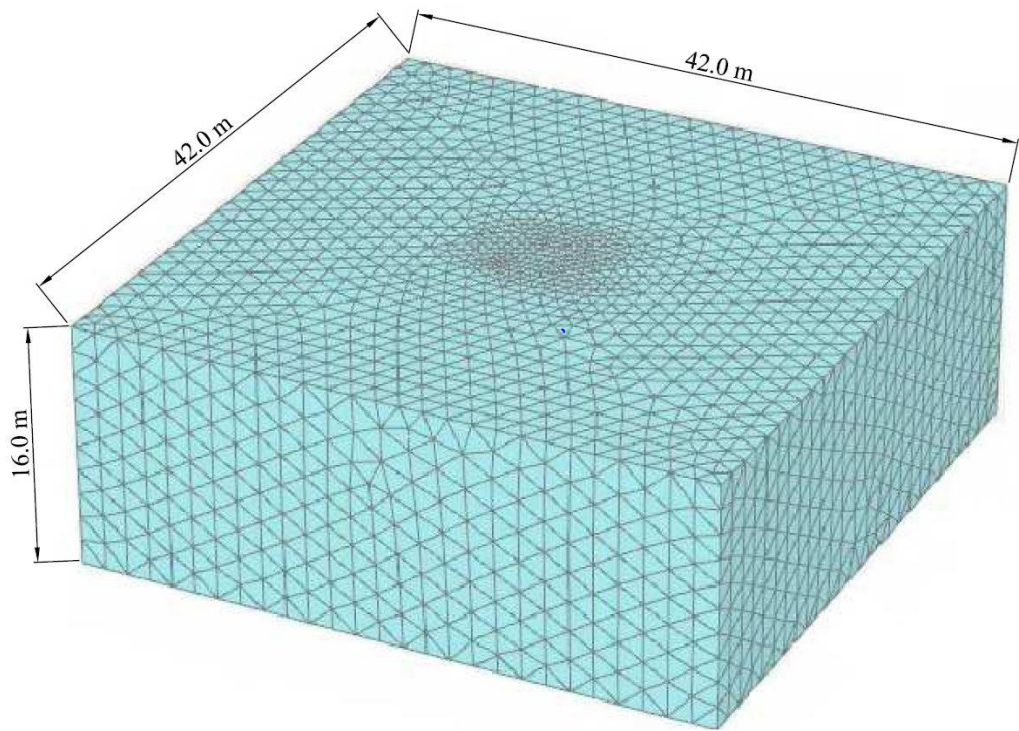

Fig. 12. Finite element model for very fine meshing in example 4.3.

It can be seen that, the present technique results are in excellent agreement with the analytical solution and more accurate than those of the FEM results with less computational effort. The deformed shape of the FE model of very fine mesh size is shown in Fig. 13.

Table 2. Displacements (m) at the center and corners of square loaded area on homogeneous elastic half space in example 4.3.

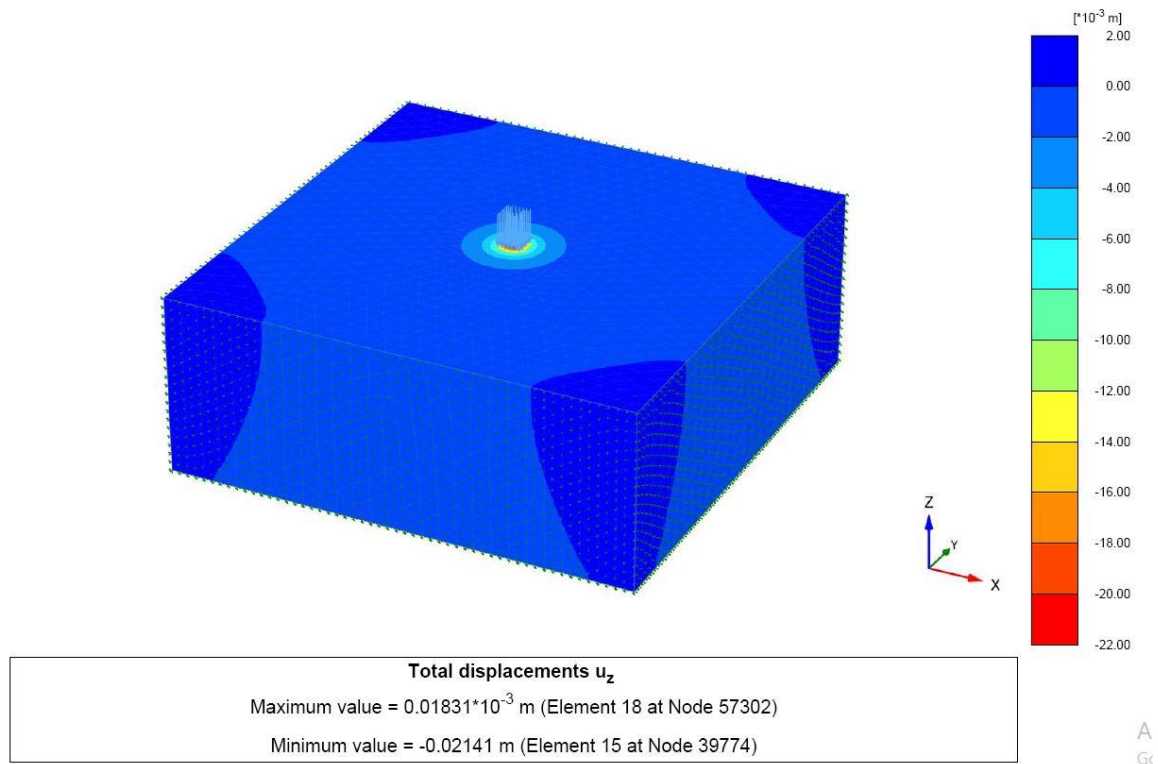|	Analytical Solution [22]	Present Mesh 1mx1m	3D FEM Medium meshing	3D FEM Fine meshing	3D FEM Very fine meshing
Center, m	0.022444	0.022238	0.01958	0.02109	0.02141
Error, %		0.92%	12.76 %	6.03 %	4.61%
Corners, m	0.011222	0.0111665	0.010223	0.01011	0.010106
Error %		0.49 %	8.9 %	9.91 %	9.94 %
Solution time, sec		42.87	255.45	530.53	1850.34

Fig. 13. Deformed shape for the finite element model of very fine meshing in example 4.3.

5. CONCLUSIONS

In this paper, a new 3D boundary element technique is presented to analyze non-homogeneous soil media. The soil media is divided into connected series of large sub-regions and zero Dirichlet BCs are considered in the far zones. Each sub-region is solved in two steps; the first one is to get the region stiffness matrix. The second one is

by postulating fixed interface nodes to compute the load vector at the interface nodes. The stiffness matrix and load vector at the interface nodes of all sub-regions are assembled. Hence, the overall system is solved to get the interface nodal displacements. Finally as a post-processing stage, each sub-region is re-solved again using the calculated region stiffness, and the computed interface nodal displacements to get the displacements and tractions at all region's nodes.

A new 3D boundary element preprocessing program is developed in order to prepare all sub-regions, elements, and nodes relevant information in a different way from those used in open source FE based preprocessing programs.

Numerical examples are solved using the presented BE technique. The results of the presented technique demonstrated excellent agreement with the analytical solution, previously published results, and the traditional finite element method with less computational effort.

The presented technique could be used as alternative to the traditional FEM to solve the overall problem of non-homogeneous soil or to be coupled with FEM to solve wide range of advanced engineering applications. In addition, the presented technique could be extended to solve plates over non-homogenous soil. As a future step, this formulation will be extended to treat non-linear soil applications.

6. ACKNOWLEDGEMENTS

DECLARATION OF CONFLICT OF INTERESTS

The authors have declared no conflict of interests.

REFERENCES

1. PLAXIS software- https://www.plaxis.com/product/plaxis-3d, (Accessed 07/03/2019)

2. Elmamlouk, H. H., Eissa, M. Y., and Hassan, A. M., "Three Dimensional Nonlinear Analysis of Vertical Single Pile Subjected to Combined Loading", Journal of Engineering and Applied Science, Vol. 57, No. 6, pp. 453-469, 2010.

3. MIDAS software- https://en.midasuser.com, (Accessed 12/03/2019)

4. Ong, Y. H., "Back Analysis of Laterally Loaded Pile Behavior using Midas/GTS to Determine Stiffness Modulus of Pile-soil Interface", Japanese Geotechnical Society Special Publication, Vol. 2, No. 35, pp. 1279-1284, 2016.

5. Wang, C. M., Chow, Y. K., and How, Y. C., "Analysis of Rectangular Thick Rafts on an Elastic Half Space", Computer and Geotechnics, Vol. 28, No. 3, pp. 161-184, 2001.

6. Chau, K. T., "Analytic Methods in Geomechanics", Taylor and Francis Group, Boca Raton, 2013.

7. Selvadurai, A. P. S., "Elastic Analysis of Soil Foundation Interaction.", Elsevier, Amsterdam, 1979.

8. Selvadurai, A. P. S., "On Boussinesq's Problem", International Journal of Engineering Science, Vol. 39, No. 3, pp. 317-322, 2001.

9. Sadek, M., and Shahrour, I., "Use of the Boussinesq Solution in Geotechnical and Road Engineering: Influence of Plasticity", Comptes Rendus Mecanique, Vol. 335, No. 9-10, pp. 516–520, 2007.

10. Bowels, J. E., "Foundation Analysis and Design." 5th Edition, McGraw-Hill, New York, 1996.

11. Shaaban, A. M., and Rashed, Y. F., "A Coupled BEM-stiffness Matrix Approach for Analysis of Shear Deformable Plates on Elastic Half Space", Engineering Analysis with Boundary Elements, Vol. 37, No. 4, pp. 699-707, 2013.

12. Small, J. C., and Booker, J. R., "Finite Layer Analysis of Layered Elastic Materials Using a Flexibility Approach, Part 1- Strip Loadings", International Journal for Numerical Methods in Engineering, Vol. 20, No. 6, pp. 1025-1037, 1984.

13. Tian, G., and Tang, L., "Extended Finite Layer Method for Semi-space Ground Analysis", Geotechnical and Geological Engineering, Vol. 35, No. 2, 1984.

14. Small, J. C., and Booker, J. R., "Finite Layer Analysis of Layered Elastic Materials using a Flexibility Approach, Part 2- Circular and Rectangular Loadings", International Journal for Numerical Methods in Engineering, Vol. 23, No. 5, pp. 959-978, 1986.

15. Maier, G., and Novati, G., "Boundary Element Elastic Analysis of Layered Soil by a Successive Stiffness Method.", International Journal for Numerical and Analytical Methods in Geomechanics, Vol. 11, No. 5, pp. 435-447, 1987.

16. Conte, E., and Dente, G., "Settlement Analysis of Layered Soil Systems by Stiffness Method", Journal of Geotechnical Engineering, Vol. 119, No. 4, pp. 780-785, 1993.

17. Kausel, E., "Generalized Stiffness Matrix Method for Layered Soils", Soil Dynamics and Earthquake Engineering, Vol. 115, pp. 663–672, 2018.
18. Xiao, S., Yue, Z. Q., and Xiao, H. T., "Boundary Element Analysis of Elastic Fields in Non-horizontally Layered Half Space whose Horizontal Boundary Subject to Tractions", Engineering Analysis with Boundary Elements, Vol. 95, pp. 105-123, 2018.
19. Pereira, A., and Parreira, P., "Direct Evaluation of Cauchy-principal-value Integrals in Boundary Elements for Infinite and Semi-infinite Three-dimensional Domains", Engineering Analysis with Boundary Elements, Vol. 13, pp. 313-320, 1994.
20. Beer, G., Smith, I., and Duenser, C., "The Boundary Element Method with Programming for Engineers and Scientists", Springer-Wien, New York, 2008.
21. Gmsh software https://www.Gmsh.info, (Accessed 10/02/2019)
22. Timoshenko, S. P., and Goodier, J.N., "Theory of Elasticity", McGraw-Hill, USA, 1970.

التمثيل ثلاثى الأبعاد للتربة الغير متجانسة باستخدام طريقة العناصر الحدودية

يقــدم البحــث أســلوب جديــد باســتخدام طريقــة العناصــر الحدوديــة لحســاب الهبــوط والإجهــادات فــي التربــة الغيــر متجانســة. وعلــى عكــس طريقــة العناصــر الحدوديــة التقليديــة فــإن الجــزء المبتكــر يــتم فيــه تقســيم التربــة تحــت منطقــة التحميــل إلــى منــاطق ثلاثيــة الأبعــاد بطريقــة العناصــر الحدوديــة وحســاب الجســاءة لكــل منطقــة علــى حــدى عنــد نقــاط الالتصــاق بــين المنــاطق ثــم تجميــع الجســاءات المحســوبة لتكــوين مصــفوفة الجســاءة الكليــة وبالتــالى يمكــن حســاب الإزاحــات عنــد نقــاط الالتصــاق بــين المنــاطق وحــل كــل منطقــة علــى حــدى باســتخدام الجســاءة والإزاحــات المحســوبة عنــد نقــاط الالتصــاق الخاصــة بالمنطقــة ونظــرا للشــكل الهندســي المعقــد للمســألة تــم عمــل برنــامج لتجهيــز كــل البيانــات اللازمــة للحــل وتؤكــد الأمثلــة المحلولــة الدقــة العاليــة للأســلوب المســتخدم مقارنــة بالنتــائج التحليلــة والنتــائج المنشــورة ســابقا وكــذلك بنتــائج طريقــة العناصــر المحددة التقليدية وبمجهود حسابى أقل.